Reviews in Aquaculture
August 2020, Volume 12, Issue 3, Pages 1783-1791
https://doi.org/10.1111/raq.12409
https://archimer.ifremer.fr/doc/00599/71161/

Non- invasive functional exploration techniques for bivalves with applications to pearl oyster *Pinctada margaritifera*

Le Moullac Gilles [1, *], Soyez Claude [1], Lyonnard Pierre [1], Chabrier Sébastien [2], Milhade Leo [1], Gueguen Yannick [3], Beliaeff Benoit [1]

[1] Ifremer UMR Ecosystèmes Insulaires Océaniens UPF ILM IRD Taravao Tahiti, Polynésie française
[2] Laboratoire GEPASUD Université de Polynésie Française Faa'a Tahiti ,Polynésie française
[3] UMR IHPE Université de Montpellier CNRS Ifremer UPVD Montpellier, France

* Corresponding author : Gilles Le Moullac, email address : gilles.le.moullac@ifremer.fr

Abstract :

Non-invasive functional exploration techniques can provide information on different aspects of general organism functioning and, unlike lethal or invasive techniques, allow individual organisms to be monitored for as long as necessary. For bivalves, a fairly wide variety of methods and instrumental means exist allowing physiology to be assessed on-line while keeping animals alive and intact. The current range of non-invasive techniques for bivalves consists of systems for measuring metabolic flows and valve activity, which can be used on bivalve molluscs for as long as an individual animal's characteristics (e.g. size) make this technically feasible. In this paper, we present some of these non-invasive techniques with applications for pearl oyster and list other potentially promising techniques. We also focus on a unique method we developed specifically for to record the pearl rotation characteristics within pearl oysters. This article presents the state of the art in non-invasive functional exploration techniques. We hope that the information provided here will be useful to physiologists of bivalve marine molluscs through the tools and applications presented here or other future approaches based on them.

Keywords : bivalve, filtration, pearl rotation, respiration, valvometry

Introduction

The pearl oyster *Pinctada margaritifera* is a marine bivalve with a distribution range in the intertropical zone of the Pacific and Indian Oceans. This species is exploited, mainly in French Polynesia, for the production of cultured pearls. For many years this species has been the subject of studies aiming to improve knowledge of its nutritional needs (Le Moullac et al., 2013; Vahirua-Lechat et al., 2008), reproduction (Chávez-Villalba et al., 2011; Teaniniuraitemoana et al., 2015, 2014) and mechanisms controlling biomineralization (Blay et al., 2018; Joubert et al., 2014, 2010; Le Luyer et al., 2019). Beyond the acquisition of purely biological knowledge*, P. margaritifera* is studied for the improvement of pearl production (Gueguen et al., 2013) and its potential to adapt to environmental challenges (Beliaeff et al., 2017). Ecophysiological approaches make it possible to study and model the behavioural and physiological responses of pearl oysters to their environment over their development, and can be based on non-invasive exploration techniques. In contrast to invasive techniques, non-invasive functional exploration allows individual organisms to be monitored as long as necessary. Such non-invasive experimental approaches can provide information on the general functioning of organisms. For bivalves, there is a fairly wide variety of methods and instrumental means allowing on-line physiological assessment of intact animals. The current range of non-invasive techniques for bivalves includes systems for measuring metabolic flows (filtration, respiration) and valve activity that can be applied to the bivalve molluscs as long as the animal characteristics (e.g. size) make this technically feasible. In this paper we present those non-invasive techniques with applications to pearl oyster, and list other potentially promising approaches. We also focus on a unique method that we developed specifically for the pearl oyster to record pearl rotation characteristics.

Measuring metabolic fluxes

In living organisms, the measurement of ecophysiological parameters of nutrition and respiration makes it possible to establish an energetic balance of assimilated organic matter. In bivalves, this balance is generally expressed as a growth potential including reproduction, known as "Scope For

Growth, SFG" (Bayne, 1976). Based on ecophysiological functions such as filtration, consumption, absorption and respiration, which are known to vary according to the environment, the energy balance provides an "estimate" of the physiological status of the animal at different periods of its development and according to the environmental parameters. More precisely, the calculation of an organism's energy balance consists in drawing up a balance of energy gains and losses, assuming that the amount of energy acquired through food during assimilation is used for maintenance, growth and reproduction. The energy balance calculation is more accurate when filtration and respiration measurements are carried out on the same animals, in the same enclosure.

Measurements of bivalve ingestion and respiration allow an energy balance to be established, providing indications about the relationship of these animals with their living conditions. In our ecophysiological measurement system (EMS) (Figure 1a) (Chávez-Villalba et al., 2013), energy flows can be measured in an, which is composed of eleven open-flow chambers. In our experiments ten oysters are placed in ten of the chambers and the remaining eleventh chamber is left empty to serve as a control. The drains of the chambers are each equipped with a two-way electromagnetic valve activated by an automaton. When the valve of one measuring chamber is opened, the released water is analyzed for 3 min using a 10AU fluorometer (Turner, USA) and an oximeter (OXI 358, WTW, Weilheim, Germany) to measure the fluorescence and dissolved oxygen. The measurements of each chamber are carried out by piloting 11 electrovans, which successively remove part of the effluent to the sensors (oximeter, fluorimeter). A National Instrument (NI) Ethernet cFP-2120 network module is controlled by a real-time LabView (NI) driver. The card transmits data and tracking graphs via Ethernet on an interface (figure 1b) that provides the values of incoming flows, sampling by successive opening and closing of the electrovans, real-time display of all curves (fluorescence of microalgae, dissolved oxygen, flows), and recording of average data on the computer dedicated to EMS management. Each cycle is completed within 3 min and another cycle then starts in the control chamber and lasts 3 min (sequence: chamber 1, control, chamber 2, control, etc.). The specimens remain in the chambers for 48 h and measurements can be taken every 60 min until 48 fluorescence

and oxygen measurements have been recorded. The respiration rate (RR), expressed in mg O_2 h^{-1}, is estimated by the difference in the oxygen concentration between the control and experimental chambers using the following formula: RR = V (O1 - O2), where O1 is the oxygen concentration in the control chamber, O2 the oxygen concentration in the experimental chamber, and V the water flow rate. Ten measurement series are commonly performed on groups of four pearl oysters, each composed of two grafted and two non-grafted pearl oysters. The energy expenditure is expressed as RR of individuals (total energy expenditure) and as standardized RR (Savina and Pouvreau, 2004).

Replicates from EMS thus make it possible to accurately estimate the energy status of the bivalves under various environmental pressures or according to their physiological status and/or genetics. Measurements are taken on individuals who have previously been acclimatized for at least one month in a contiguous room with 8 500 L tanks also equipped with environmental control systems. This experimental tool allowed us to show that the oxygen requirement of female *P. margaritifera* is higher than that of males (Chávez-Villalba et al., 2013). The energy balance of the species was also measured at different temperatures to calculate its thermal optimum and to estimate the energy risk of climate warming (Le Moullac et al., 2016a); this also demonstrated that acidification has no significant impact (Le Moullac et al., 2016b). The effect of anthropogenic environmental pressures such as microplastics has been studied and we have thus been able to determine that the bioenergetic response is dose-dependent (Gardon et al., 2018). Finally, we observed that pearl oysters grafted for the production of cultured pearls did not expend significatively more energy, as estimated by oxygen consumption, than the non-grafted ones. We could therefore inferred that the energy cost associated with pearl formation is negligible (Le Moullac et al., 2018b).

Measuring pearl rotation

Cultured pearls are produced by first making a grafting operation, during which a small piece of mantle tissue from a donor oyster (the graft) is inserted in the gonad of the recipient oyster together with a nacre bead, the nucleus (Wada, 1999). Once positioned in the recipient oyster, the outer

epithelium cells of the graft multiply and form a pearl sac around the nucleus. The pearl sac then starts to deposit nacre (aragonite) layers onto the nucleus. This is the starting point of the future pearl. A rearing period of approximately 18 months is then needed to produce a pearl with a sufficiently thick layer of nacre for the market (Gueguen et al., 2013). A pearl is round for at least two reasons: (i) because the nucleus is spherical and (ii) the growth front of nacre on the surface of the pearls suggests that rotation is taking place. Cartwright et al. (2013) put forward a theory of pearl rotation, explaining how forces acting during the deposition of aragonite tablets would lead to a particular type of pearl movement. The layers of aragonite oriented in specific directions on the surface would give momentum to the pearl during the growth of its layers, thus causing movement. Once activated, a dynamic mechanism would be initiated that could lead to different rotational movements, particularly depending on whether the pearl has a defect. We were finally able to develop an unique device to make demonstrate that the pearl rotates during its formation in the pearl sac of the pearl oyster *Pinctada margaritifera* (Gueguen et al., 2015).

The magnetometer used in this study is made up of three main connected parts. The measuring part is a dome with sensors consisting of a half-sphere of acrylic glass (diameter 20 cm) on which are set 25 magnetic sensors each consisting of two components (figure 2), an HMC1021 compass from Honeywell (a one-axis magnetic sensor) and an offset compensation circuit. Twenty-four of the 25 sensors are spread across the convex surface of the dome in three circles of eight elements at 0°, 30° and 60° angles with the base. The last sensor is located at the top of the dome at 90°. Each sensor is glued on the dome with a cyanoacrylate paste and protected from impacts and water by an acrylic glass tube. The electrical part of the magnetometer is composed of a data acquisition board with 26 RJ45 sockets (25 used to connect the cables from the sensors and the last one to make the ethernet connection with the computer) and 25 wiring cables, each of which ends in a RJ45 plug. The Human-Machine Interface (HMI) is a program called “magneto”, developed by VEGA Industrie (Avrainville, France), which is composed of two parts. The first part of the HMI is a microcontroller that uses internal software to collect, process and transfer data to the second. This second part is software on

133 the computer (magneto-magnetometer interface 1.0), which collects data from the microcontroller,
134 allows data to be collected from real time sensors and produces visualized data, thus tracking the
135 acquisition process. This interface is used to define communication, data acquisition parameters and
136 to make backups. The following parameters were defined for our experiments: acquisition frequency:
137 50 (1/10s); filtration rate: 5; recording periodicity: 1 minute. The export data file is a .CSV file, which
138 the software names with references to the date and hour of start:
139 Magneto_YYYY_MM_DD_HH_MM.csv. The data acquired by the magnetometer were processed with
140 an R routine to convert the data acquired into 3D coordinates and perform calculations on pearl
141 movement kinetics. Mean angular speed of rotation (min^{-1}) and a graphical representation
142 determining the type of pearl motion could then be derived from the converted data (figure 3).

143 The experiment carried out using this device showed that the pearl actually turns in the pearl sac,
144 with rotation starting as soon as the pearl sac closes (Gueguen et al., 2015). The pearl sac is the result
145 of the development of cells of the graft that was implanted during the grafting operation, at the
146 same time as the nucleus. The healing of the gonad and development of the pearl sac take time. It is
147 estimated that the pearl sac becomes functional – i.e., the first aragonite deposits are observed –
148 between 30 and 45 days after the transplant operation. This was confirmed by rotational recordings
149 using a magnetometer in pearl oysters grafted with magnetized nuclei (Gueguen et al., 2015).

150 Once the rotation of pearls was demonstrated, the question of most interest to the industry was the
151 link between rotation and formation, and hence quality, of pearls. We first showed that rotation
152 speed differed according to the type of movement: pearls with axial movement had a significantly
153 higher rotation speed than those with random movement (Le Moullac et al, 2018a). When we
154 conducted ecophysiological experiments to test the impact of the environment on pearl rotation and
155 formation, however, we found pearl growth rate to be influenced by temperature but not by pearl
156 rotation speed. On the basis of our results, we now consider pearl rotation to be a more complex
157 process than formerly thought. Mechanisms involved could include strong environmental forcing in

158 immediate proximity to the pearl. Another implication of our findings is that, in the context of ocean
159 warming, pearl growth and quality can be expected to decrease in pearl oysters exposed to
160 temperatures above 30°C (Le Moullac et al., 2018a).

161 Measuring valve activity

162 Bivalve valve behaviour is a potentially important tool for biological monitoring of water quality as,
163 through these movements, bivalves can serve as environmental sentinels (Borcherding, 2006). Valve
164 activity is also essential for understanding metabolism optimization strategies. A relatively large
165 number of methods exist for observing and measuring valve movement, as presented below.

166 A strain gauge can be used to record valve movements of oysters. Composed of electrically resistant
167 wires, it converts the stretching of these wires into variations in electrical resistance. Strain gauges
168 are cemented onto thin, flexible strips of metal that are attached to a nylon line. This line is
169 cemented onto the upper valve of the oyster. A system of this type (BLH Electronics, Waltham,
170 Mass., U.S.A.) was developed to measure shell-valve gape activity and periodic activity of *Crassostrea*
171 *virginica* (Higgins, 1980). It was later applied to mussels following their exposure to the toxic
172 dinoflagellate *Protogonyaulax tamarensis* (Shumway and Cucci, 1987). Subsequently, Porter and
173 Breitburg (2016) developed a comparable system (SG13/1000–LY43 or LY41, Omega Engineering Inc.,
174 Stanford, Connecticut) directly sealed onto the shells for gape monitoring of *C virginica* under diel-
175 cycling hypoxia.

176 An inductance-based valvometry device was constructed to study the valve rhythm dynamics of
177 *Corbicula fluminae* when exposed to copper (Jou et al., 2016). This device was conceived by attaching
178 a pair of lightweight electrical coils to the valves and using them as sensors to determine the degree
179 of bivalve opening. This system makes it possible to record the valve behaviour of several bivalves
180 simultaneously. An interface card (NI DAQPad-6259) controls the acquisition of the corresponding
181 signals, and a specific LabVIEW program monitor compiles data. This way, valve activities of clams
182 were recorded dynamically in real time.

183 The HFNI valvometer is a high frequency (10 Hertz), non-invasive (HFNI) biosensor. The animal is
184 equipped with two light coils (sensors), ≈53 mg each (unembedded), fixed on the edge of each valve.
185 These coils are coated with a resin-sealing before fixation to the valves. One of the coils emits a high-
186 frequency sinusoidal signal that is received by the other coil. Each animal's behaviour is thus
187 measured every 1.6 s (Andrade et al., 2016; Sow et al., 2011).

188 Gaping activity is measured using magnetoresistive sensors (Honeywell). The sensor is formed by
189 four encapsulated reeds activated by a magnet, and the supports glued onto each valve. The magnet
190 is also encapsulated, with the reeds and slides hanging on it attached to two stainless steel rods of 1
191 mm diameter and 10 cm long (Garcia-March et al., 2016).

192 In our laboratory, a type of electromagnetic valvometer was tested. This is an automatic and
193 continuous recording device of bivalve valve movements designed according to the Hall Effect
194 Principle (1879), which states that an electric current passing through a material bathed in a
195 magnetic field generates a voltage perpendicular to the latter. The valvometer ("Mémocollecteur"
196 developed by Micrel, Hennebont, Morbihan), described by Floch (1994), takes the form of cylindrical
197 structure of approximately 300 mm in diameter, with a maximum height of 50 mm and a mass of 2
198 kg. Between 4 and 8 bivalves are fixed horizontally in the periphery on a PVC crown, while the centre
199 of the device contains an autonomous miniaturized data acquisition microprocessor. The PVC blades
200 come out from a receptor, and reach onto the top valve of the oysters, opposite the hinge. An
201 adjustable vinyl tip adjusts the sensor position when the oyster is closed. When the oyster opens, the
202 tip lifts the PVC blade. The gap between the stem and the central receptor thus increases. An
203 electromagnet located in this receptor transforms this gap into an electrical signal.

204 When the signal is part of a time series (figure 4), spectral analysis can reveal the rhythms of activity.
205 In our study, spectral analysis of the record series of the valved activity revealed a period of 23.25 h
206 and a lower density of 2.15 h (figure 5a), followed by a set of repetitive high-frequency and low-
207 amplitude micro-movements (figure 5b). These micro-movements are interesting because they were

208 almost perpetual. These micromovements could be one of the engines of filtration, in addition to the
209 ciliary activity of the gills. Correspondingly, we can now hypothesize that these valve micromotions
210 are involved in the rotation of beads in grafted pearl oysters. This hypothesis should be tested by
211 simultaneously measuring the valve activity and the rotation of the bead at the same frequency (per
212 second). In *P. margaritifera*, the records of pearl oyster valve opening variations over 15 days in the
213 lagoon of Takapoto in 1995 (Buestel, unpublished data) revealed a marked diel cycle. Oysters open
214 more, and thus filter more, at night than during the day.

215 The valvometers put out an electrical signal (mV) that is used in a binary manner (open/closed),
216 together with the opening time (Jou et al., 2016; Porter and Breitburg, 2016), or transformed into a
217 spread value (mm). The spread value of the opened valves can be compared when the
218 measurements are standardized; in this case, the opening width (mm) is transformed into the degree
219 of aperture considering the valves as two sides of a right-angled triangle. The spread of the opening
220 is then the measure on the opposite side of the angle, transformed into an aperture angle. Indeed,
221 the height, unlike the angle, depends on the position of the needle on the animal and the animal's
222 length. To eliminate this bias, by likening the oyster to a right-angled triangle (figure 6), it is then
223 possible to calculate: $\sin(\alpha) = H/L$, hence $\alpha = \arcsin(H/L)$. In a previous study (Le Moullac, 2008), this
224 transformation of valve spread values made it possible to measure responses to prolonged hypoxia
225 in Pacific oyster *C. gigas*, which induced a reduction in average valve opening.

226 Non-invasive methods for future applications

227 Measuring cardiac activity could usefully complement the range of different measures described
228 above. Heart rate was successfully used as a proxy for whole-animal stress (Braby and Somero,
229 2006), in response to toxins (Davenport, 1977; Depledge et al., 1996; Grace and Gainey, 1987;
230 Wedderburn et al., 2000), temperature (Coleman and Trueman, 1971; Helm and Trueman, 1967;
231 Pickens, 1965), salinity (Nicholson, 2002; Stickle and Sabourin, 1979) and predation (Rovero et al.,
232 1999). Two main technical principles are used: impedance and infrared. Impedance, measuring an
233 electrical resistance, can be considered as an invasive technique because it requires drilling into the

bivalve shell to insert two small electrodes (copper or platinum) into the pericardial cavity. These electrodes are attached to the shell by a surgical glue or dental cement. This method produces an analogue impedance signal, which is converted to a voltage signal (Braby and Somero, 2006; Earll, 1975; Gainey and Shumway, 1988). The method of measuring heart rate (HR) by infra-red (IR) is more recent and non-invasive because it does not require perforation of the shell. A waterproof photoplethysmograph is glued on the shell in the vicinity of the cardiac region, with optical sensors consisting of an infrared transmitter and a phototransistor. Tests of the transmission of an infrared signal through the pearl oyster shell demonstrated the a limitation of the method, however, because the shells of *P. margaritifera* individuals greater than 85 mm in height are too thick to allow the IR signal through.

Magnetic resonance imaging (MRI), although not greatly used, can provide a very wide range of information that is currently acquired by bivalve dissection. Application of MRI is possible in marine bivalves, especially oysters, with sufficient spatial resolution to depict anatomy without movement artefacts or magnetic susceptibilities (Pouvreau et al., 2006). MRI techniques have been used to characterize gonad development and to determine the sex of live Pacific oysters through their shells (Davenel et al., 2009, 2006). Recent advances in MRI in real time allow us to visualize the movements of organs such as the human heart, tongue, and joints (Uecker et al., 2010; Zhang et al., 2010) (https://www.independent.co.uk/news/health/realtime-mri-live-video-tongue-jens-frahm-max-planck-institute-european-patent-office-a8327001.html). Applying such technology to the pearl oyster would allow the observation of pearl formation and improve our understanding of the origin of pearl rotation.

Conclusion

MRI exploration can provide regular information for tracking reproduction, through maturation to spawning, and to see the first developments of the pearl sac. The latest advances in MRI, which show the dynamic capabilities of real time MRI, should help to unravel some of the mystery about pearl rotation. Simultaneous non-invasive functional explorations can be considered, combining measures

of metabolic flux, rotation of pearls, and recording of valve activity, preferentially using stress gauges that would not interfere with the magnetometric system signals. This article reviews the state of the art of non-invasive functional exploration techniques that can be used in bivalves. We hope that this paper will be useful to physiologists of bivalve marine molluscs through the tools and applications presented here or others that could be conceived in the future.

Acknowledgments

The authors express their gratitude to Bélinda Hui who helped lay down the principles of the magnetometer project and Max Mastail, now retired, who led the design of the magnetometer. We also thank Dominique Buestel for providing the valvometric data. We would also like to thank the entire technical team of the Ifremer Pacific Centre (IMA team) who assembled these unique systems.

References

Andrade, H., Massabuau, J.-C., Cochrane, S., Ciret, P., Tran, D., Sow, M., Camus, L., 2016. High Frequency Non-invasive (HFNI) Bio-Sensors As a Potential Tool for Marine Monitoring and Assessments. Frontiers in Marine Science 3. https://doi.org/10.3389/fmars.2016.00187

Bayne, B.L., 1976. Aspects of reproduction in bivalve molluscs., in: WILEY, M. (Ed.), Estuarine Processes. Academic Press, pp. 432 – 448. https://doi.org/10.1016/B978-0-12-751801-5.50043-5

Beliaeff, B., Le Moullac, G., Saulnier, D., Ky, C.-L., 2017. Perliculture en Polynésie française - Enjeux économiques, scientifiques et techniques. TI base documentaire : TIB140DUO., 18.

Blay, C., Planes, S., Ky, C.-L., 2018. Cultured Pearl Surface Quality Profiling by the Shell Matrix Protein Gene Expression in the Biomineralised Pearl Sac Tissue of Pinctada margaritifera. Marine Biotechnology. https://doi.org/10.1007/s10126-018-9811-y

Borcherding, J., 2006. Ten Years of Practical Experience with the Dreissena-Monitor, a Biological Early Warning System for Continuous Water Quality Monitoring. Hydrobiologia 556, 417–426. https://doi.org/10.1007/s10750-005-1203-4

Braby, C.E., Somero, G.N., 2006. Following the heart: temperature and salinity effects on heart rate in native and invasive species of blue mussels (genus Mytilus). Journal of Experimental Biology 209, 2554–2566. https://doi.org/10.1242/jeb.02259

Cartwright, J.H.E., Checa, A.G., Rousseau, M., 2013. Pearls Are Self-Organized Natural Ratchets. Langmuir 29, 8370–8376. https://doi.org/10.1021/la4014202

Chávez-Villalba, J., Soyez, C., Aurentz, H., Le Moullac, G., 2013. Physiological responses of female and male black-lip pearl oysters *(Pinctada* margaritifera) to different temperatures and concentrations of food. Aquatic Living Resources 26, 263–271. https://doi.org/10.1051/alr/2013059

Chávez-Villalba, J., Soyez, C., Huvet, A., Gueguen, Y., Lo, C., Le Moullac, G., 2011. Determination of gender in the pearl oyster Pinctada margaritifera. Journal of Shellfish Research 30, 231–240.

296 Coleman, N., Trueman, E.R., 1971. The effect of aerial exposure on the activity of the mussels Mytilus
297 edulis L. and Modiolus modiolus (L.). Journal of Experimental Marine Biology and Ecology 7,
298 295–304. https://doi.org/10.1016/0022-0981(71)90011-6
299 Davenel, A., Pouvreau, S., Cambert, M., Suquet, M., Mariette, F., 2009. NMR relaxometry as a
300 potential non-invasive routine sensor for characterization of phenotype in Crassostrea gigas.
301 Aquaculture 291, 74–77. https://doi.org/10.1016/j.aquaculture.2009.03.008
302 Davenel, A., Quellec, S., Pouvreau, S., 2006. Noninvasive characterization of gonad maturation and
303 determination of the sex of Pacific oysters by MRI. Magnetic Resonance Imaging 24, 1103–
304 1110. https://doi.org/10.1016/j.mri.2006.04.014
305 Davenport, J., 1977. A study of the effects of copper applied continuously and discontinuously to
306 specimens of *Mytilus edulis* (L.) exposed to steady and fluctuating salinity levels. Journal of
307 the Marine Biological Association of the United Kingdom 57, 63–74.
308 https://doi.org/10.1017/S0025315400021238
309 Depledge, M.H., Lundebye, A.-K., Curtis, T., Aagaard, A., Andersen, B.B., 1996. Automated interpulse-
310 duration assessment (AIDA): a new technique for detecting disturbances in cardiac activity in
311 selected macroinvertebrates. Marine Biology 126, 313–319.
312 https://doi.org/10.1007/BF00347455
313 Earll, R., 1975. Temporal variation in the heart activity of Scrobicularia plana (Da Costa) in constant
314 and tidal conditions. Journal of Experimental Marine Biology and Ecology 257–274.
315 Floch, A., 1994. Un capteur biologique original enregistrant les mouvements valvaires des mollusques
316 bivalves (PhD Thesis). Ecole nationale vétérinaire, Nantes.
317 Gainey, L.F., Shumway, S.E., 1988. Physiological effects of Protogonyaulax tamarensis on cardiac
318 activity in bivalve molluscs. Comparative Biochemistry and Physiology Part C: comparative
319 pharmacology 159-164.
320 Garcia-March, J.R., Jiménez, S., Sanchis, M.A., Monleon, S., Lees, J., Surge, D., Tena-Medialdea, J.,
321 2016. In situ biomonitoring shows seasonal patterns and environmentally mediated gaping
322 activity in the bivalve, Pinna nobilis. Marine Biology 163. https://doi.org/10.1007/s00227-
323 016-2812-3
324 Gardon, T., Reisser, C., Soyez, C., Quillien, V., Le Moullac, G., 2018. Microplastics Affect Energy
325 Balance and Gametogenesis in the Pearl Oyster *Pinctada margaritifera*. Environmental
326 Science & Technology 52, 5277–5286. https://doi.org/10.1021/acs.est.8b00168
327 Grace, A.L., Gainey, L.F., 1987. The Effects of Copper on the Heart Rate and Filtration Rate of Mytilus
328 edulis. Marine Pollution Bulletin 87–91.
329 Gueguen, Y., Czorlich, Y., Mastail, M., Le Tohic, B., Defay, D., Lyonnard, P., Marigliano, D., Gauthier, J.-
330 P., Bari, H., Lo, C., Chabrier, S., Le Moullac, G., 2015. Yes, it turns: experimental evidence of
331 pearl rotation during its formation. Royal Society Open Science 2, 150144.
332 https://doi.org/10.1098/rsos.150144
333 Gueguen, Y., Montagnani, C., Joubert, C., Marie, B., Belliard, C., Tayale, A., Fievet, J., Levy, P.,
334 Piquemal, D., Marin, F., Le Moullac, G., Ky, C.-L., Garen, P., Lo, C., Saulnier, D., 2013.
335 Characterization of molecular processes involved in the pearl formation in *Pinctada*
336 margaritifera for a sustainable development of pearl farming industry in French Polynesia, in:
337 Watabe, S., Maeyama, K., Nagasawa, H. (Eds.), Recent Advances in Pearl Research.
338 TERRAPUB, pp. 183–195.
339 Helm, M.M., Trueman, E.R., 1967. The effect of exposure on the heart rate of the mussel, Mytilus
340 edulis L. Comparative Biochemistry and Physiology 21, 171–177.
341 https://doi.org/10.1016/0010-406X(67)90126-0
342 Higgins, P.J., 1980a. Effects of food availability on the valve movements and feeding behavior of
343 juvenile Crassostrea viginica (Gmelin). I. Valve movements and periodic activity. Journal of
344 Experimental Marine Biology and Ecology 48, 229–244.
345 Higgins, P.J., 1980b. EFFECTS OF FOOD AVAILABILITY ON THE VALVE MOVEMENTS AND FEEDING
346 BEHAVIOR OF JUVENILE CRASSOSTREA VIRGINICA (Gmelin). 11. FEEDING RATES AND
347 BEHAVIOR. Journal of Experimental Marine Biology and Ecology 46, 17–27.

348 Jou, L.-J., Chen, B.-C., Chen, W.-Y., Liao, C.-M., 2016. Sensory determinants of valve rhythm dynamics
349 provide in situ biodetection of copper in aquatic environments. Environmental Science and
350 Pollution Research 23, 5374–5389. https://doi.org/10.1007/s11356-015-5735-5
351 Joubert, C., Linard, C., Le Moullac, G., Soyez, C., Saulnier, D., Teaniniuraitemoana, V., Ky, C.L.,
352 Gueguen, Y., 2014. Temperature and Food Influence Shell Growth and Mantle Gene
353 Expression of Shell Matrix Proteins in the Pearl Oyster Pinctada margaritifera. PLoS ONE 9,
354 e103944. https://doi.org/10.1371/journal.pone.0103944
355 Joubert, C., Piquemal, D., Marie, B., Manchon, L., Pierrat, F., Zanella-Cléon, I., Cochennec-Laureau, N.,
356 Gueguen, Y., Montagnani, C., 2010. Transcriptome and proteome analysis of *Pinctada*
357 margaritifera calcifying mantle and shell: focus on biomineralization. BMC genomics 11, 613.
358 Le Luyer, J., Auffret, P., Quillien, V., Leclerc, N., Reisser, C., Vidal-Dupiol, J., Ky, C.-L., 2019. Whole
359 transcriptome sequencing and biomineralization gene architecture associated with cultured
360 pearl quality traits in the pearl oyster, Pinctada margaritifera. BMC Genomics 20.
361 https://doi.org/10.1186/s12864-019-5443-5
362 Le Moullac, G., 2008. Adaptation du métabolisme respiratoire de l'huître creuse Crassostrea gigas
363 (PhD thesis). Université de Caen Basse-Normandie, Caen.
364 Le Moullac, G., Schuck, L., Chabrier, S., Belliard, C., Lyonnard, P., Broustal, F., Soyez, C., Saulnier, D.,
365 Brahmi, C., Ky, C.-L., Beliaeff, B., 2018a. Influence of temperature and pearl rotation on
366 biomineralization in the pearl oyster, *Pinctada margaritifera*. The Journal of Experimental
367 Biology 221, jeb186858. https://doi.org/10.1242/jeb.186858
368 Le Moullac, G., Soyez, C., Ky, C.-L., 2018b. Low energy cost for cultured pearl formation in grafted
369 chimeric Pinctada margaritifera. Scientific Reports 8. https://doi.org/10.1038/s41598-018-
370 25360-5
371 Le Moullac, G., Soyez, C., Latchere, O., Vidal-Dupiol, J., Fremery, J., Saulnier, D., Lo Yat, A., Belliard, C.,
372 Mazouni-Gaertner, N., Gueguen, Y., 2016a. Pinctada margaritifera responses to temperature
373 and pH: Acclimation capabilities and physiological limits. Estuarine, Coastal and Shelf Science
374 182, 261–269. https://doi.org/10.1016/j.ecss.2016.04.011
375 Le Moullac, G., Soyez, C., Sham-Koua, M., Levy, P., Moriceau, J., Vonau, V., Maihota, M., Cochard,
376 J.C., 2013. Feeding the pearl oyster *Pinctada* margaritifera during reproductive conditioning.
377 Aquaculture Research 44, 404–411. https://doi.org/10.1111/j.1365-2109.2011.03045.x
378 Le Moullac, G., Soyez, C., Vidal-Dupiol, J., Belliard, C., Fievet, J., Sham Koua, M., Lo Yat, A., Saulnier,
379 D., Gaertner-Mazouni, N., Gueguen, Y., 2016b. Impact of pCO2 on the energy, reproduction
380 and growth of the shell of the pearl oyster Pinctada margaritifera. Estuarine, Coastal and
381 Shelf Science 182, 274–282. https://doi.org/10.1016/j.ecss.2016.03.011
382 Nicholson, S., 2002. Ecophysiological aspects of cardiac activity in the subtropical mussel Perna viridis
383 (L.) (Bivalvia: Mytilidae). Journal of Experimental Marine Biology and Ecology 267, 207–222.
384 https://doi.org/10.1016/S0022-0981(01)00362-8
385 Pickens, P.E., 1965. Heart Rate of Mussels as a Function of Latitude, Intertidal Height, and
386 Acclimation Temperature. Physiological Zoology 38, 390–405.
387 https://doi.org/10.1086/physzool.38.4.30152416
388 Porter, E.T., Breitburg, D.L., 2016. Eastern oyster, Crassostrea virginica, valve gape behavior under
389 diel-cycling hypoxia. Marine Biology 163. https://doi.org/10.1007/s00227-016-2980-1
390 Pouvreau, S., Rambeau, M., Cochard, J.C., Robert, R., 2006. Investigation of marine bivalve
391 morphology by in vivo MR imaging: First anatomical results of a promising technique.
392 Aquaculture 259, 415–423. https://doi.org/10.1016/j.aquaculture.2006.05.018
393 Rovero, F., Hughes, R.N., Chelazzi, G., 1999. Cardiac and behavioural responses of mussels to risk of
394 predation by dogwhelks. Animal Behaviour 58, 707–714.
395 https://doi.org/10.1006/anbe.1999.1176
396 Savina, M., Pouvreau, S., 2004. A comparative ecophysiological study of two infaunal filter-feeding
397 bivalves: Paphia rhomboïdes and Glycymeris glycymeris. Aquaculture 239, 289–306.
398 https://doi.org/10.1016/j.aquaculture.2004.05.029

399 Shumway, S.E., Cucci, T.L., 1987. The effects of the toxic dinoflagellate Protogonyaulax tamarensis on
400 the feeding and behaviour of bivalve molluscs. Aquatic Toxicology 10, 9–27.
401 Sow, M., Durrieu, G., Briollais, L., Ciret, P., Massabuau, J.-C., 2011. Water quality assessment by
402 means of HFNI valvometry and high-frequency data modeling. Environmental Monitoring
403 and Assessment 182, 155–170. https://doi.org/10.1007/s10661-010-1866-9
404 Stickle, W.B., Sabourin, T.D., 1979. Effects of salinity on the respiration and heart rate of the common
405 mussel, Mytilus edulis L., and the black chiton, Katherina tunicata (Wood). Journal of
406 Experimental Marine Biology and Ecology 41, 257–268. https://doi.org/10.1016/0022-
407 0981(79)90135-7
408 Teaniniuraitemoana, V., Huvet, A., Levy, P., Gaertner-Mazouni, N., Gueguen, Y., Le Moullac, G., 2015.
409 Molecular Signatures Discriminating the Male and the Female Sexual Pathways in the Pearl
410 Oyster Pinctada margaritifera. PLOS ONE 10, e0122819.
411 https://doi.org/10.1371/journal.pone.0122819
412 Teaniniuraitemoana, V., Huvet, A., Levy, P., Klopp, C., Lhuillier, E., Gaertner-Mazouni, N., Gueguen, Y.,
413 Le Moullac, G., 2014. Gonad transcriptome analysis of pearl oyster Pinctada margaritifera:
414 identification of potential sex differentiation and sex determining genes. BMC genomics 15,
415 491.
416 Uecker, M., Zhang, S., Voit, D., Karaus, A., Merboldt, K.-D., Frahm, J., 2010. Real-time MRI at a
417 resolution of 20 ms. NMR in Biomedicine 23, 986–994. https://doi.org/10.1002/nbm.1585
418 Vahirua-Lechat, I., Laure, F., LeCoz, J.R., Bianchini, J.P., Bellais, M., Le Moullac, G., 2008. Changes in
419 fatty acid and sterol composition during oogenesis in the pearl oyster *Pinctada* margaritifera.
420 Aquaculture Research 39, 1739–1746. https://doi.org/10.1111/j.1365-2109.2008.02050.x
421 Wada, K., 1999. Formation and Quality of Pearls. Journal of Gemmological Society of Japan 20, 47–
422 62.
423 Wedderburn, J., McFadzen, I., Sanger, R.C., Beesley, A., Heath, C., Hornsby, M., Lowe, D., 2000. The
424 Field Application of Cellular and Physiological Biomarkers, in the Mussel Mytilus edulis, in
425 Conjunction with Early Life Stage Bioassays and Adult Histopathology. Marine Pollution
426 Bulletin 40, 257–267. https://doi.org/10.1016/S0025-326X(99)00214-3
427 Zhang, S., Uecker, M., Voit, D., Frahm, J., 2010. Real-time MRI at 20 millisecond resolution. European
428 Congress of Radiology. https://doi.org/10.1594/ecr2010/c-3415
429

430

Figure captions

Figure 1: (a) the ecophysiological measurement system (EMS) for pearl oysters *Pinctada margaritifera*, biodeposits are harvested for analysis of organic matter assimilation; b) software interface showing the lights corresponding to the metabolic chamber being analyzed (b1), simultaneous measurements of dissolved oxygen and microalgae fluorescence (b2).

Figure 2 : Overview of the magnetometer system. For data acquisition, a grafted pearl oyster *Pinctada margaritifera* is placed into the dome.

Figure 3 : Three-dimensional representation of the nucleus movement in two *P. margaritifera* pearl oysters. The circular motion observed on the left pearl corresponds to a pearl whose shape is not perfectly spherical rotating on an axis. The random movement observed on the right pearl corresponds to a perfectly spherical pearl. The temporal dynamics of pearl movement are revealed by the coloration of the line illustrating the movement. The color code is that of the rainbow, the beginning of the recording is marked by the color red

Figure 4: Continuous recording of the valve activity of a pearl oyster for 17 days.

Figure 5: Spectral analysis of the continuous recording of valve activity (a) spectrogram revealing a major peak of activity at 23.25h, (b) series enlargement showing high frequency micromovements.

Figure 6 : Schematic pearl oyster whose valve opening is likened to a right-angled triangle where is the opening angle at the hinge, L: the length of the shell, H: the valve spread value opposite the hinge.

455

456

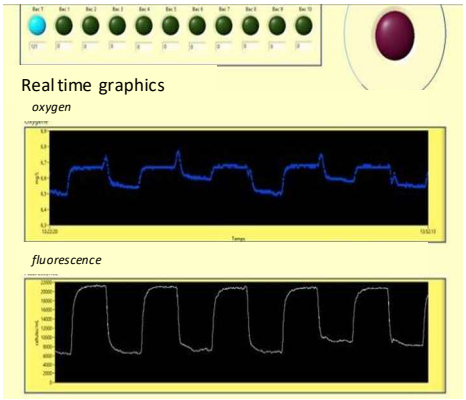

457

458 Figure 1

459

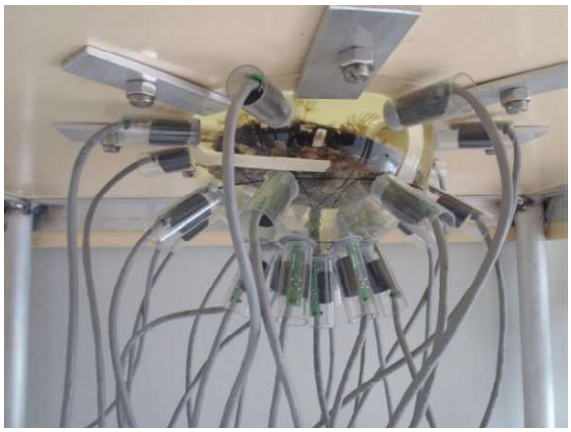

Figure 2

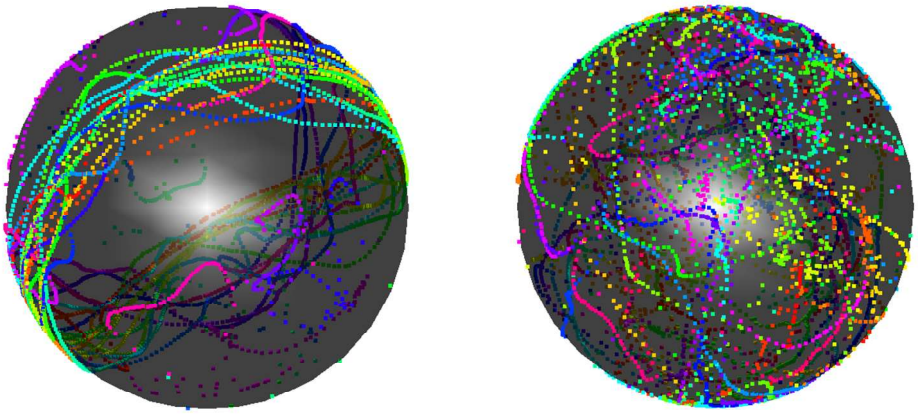

Figure 3

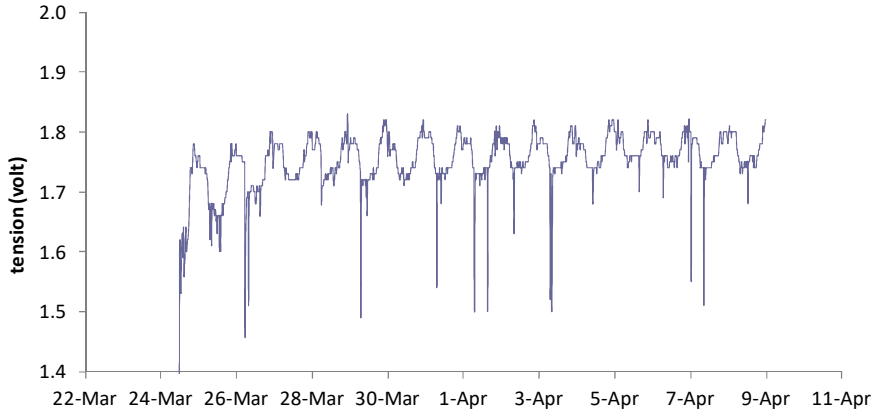

Figure 4

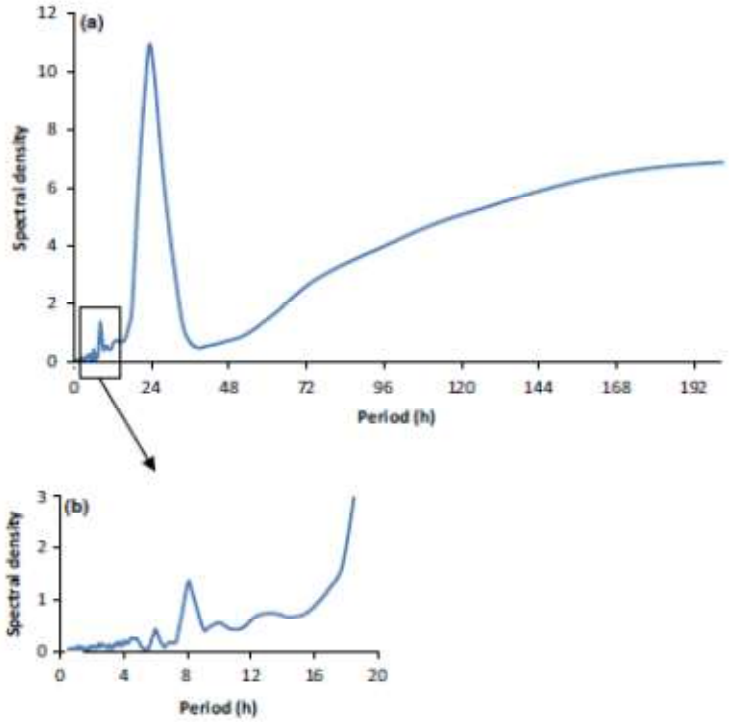

Figure 5

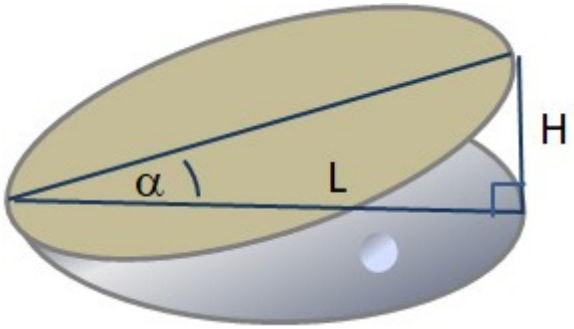

Figure 6